# Heterogeneous Fenton-like catalyst for treatment of rhamnolipid-solubilized hexadecane wastewater

Yang Liu [a,b,1], Min Cheng [a,b,1], Zhifeng Liu [a,b,1], Guangming Zeng [a,b,*], Hua Zhong [a,b,c*], Ming Chen [a,b], Chengyun Zhou[a,b], Weiping Xiong[a,b], Binbin Shao[a,b], Biao Song[a,b]

[a] *College of Environmental Science and Engineering, Hunan University, Changsha, Hunan 410082, China*

[b] *Key Laboratory of Environmental Biology and Pollution Control (Hunan University), Ministry of Education, Changsha, Hunan 410082, China*

[c] *State Key Laboratory of Water Resources and Hydropower Engineering Science, Wuhan University, Wuhan 430070, China*

Accepted MS

* Corresponding author at: College of Environmental Science and Engineering, Hunan University, Changsha, Hunan 410082, China.

E-mail address: zgming@hnu.edu.cn (G.M. Zeng), zhonghua@hnu.edu.cn (H. Zhong).

Tel.: +86–731– 88822754; fax: +86–731–88823701.

1 These authors contribute equally to this article.

**Abstract**

The treatment of wastewater containing hydrophobic organic pollutants solubilized by surfactants is of great environmental importance. In this work, the removal of rhamnolipid-solubilized hexadecane via a salicylic acid-methanol-acetone modified steel converter slag (SMA-SCS) catalyzed Fenton-like process was studied. First, we investigated the adsorption of rhamnolipid and hexadecane onto SCS and SMA-modified SCS. Compared to that of SCS, SMA-SCS exhibited better adsorption performance with maximum adsorption capacities of 0.23 and 0.28 mg/g for hexadecane and rhamnolipid, respectively. Degradation experiments showed that hexadecane was more readily degraded by the Fenton-like process than rhamnolipid. Up to 81.1% of hexadecane removal was achieved over 20 g/L of SMA-SCS within 24 h, whereas only 36% of rhamnolipid was degraded. On the other hand, the results indicated that increased rhamnolipid concentration had a negative effect on the degradation of hexadecane. During the oxidation reaction, the pH value of solution remained between 6.0 and 6.72. All these results demonstrated that the SMA-SCS/$H_2O_2$ Fenton-like process could be a cost-effective and promising approach for the treatment of surfactant-solubilized hydrophobic organic compounds.

**Keywords**: Biosurfactant; Hydrophobic organic compounds; Fenton-like; Hydroxyl radical.

Accepted MS

## 1. Introduction

The extent of anthropogenic pollution of the groundwater and soil by hydrophobic organic compounds (HOCs) is well documented. The effects of these contaminants on the ecosystem and human health and their fates are of considerable concern owing to their widespread occurrence, recalcitrance in the environment, and suspected mutagenic and carcinogenic properties (Cui et al., 2013; Cossaboon et al., 2019). Numerous studies have addressed the efficient removal of HOCs from contaminated sites (Lin et al., 2009; Wu et al., 2018). However, due to their low aqueous solubility, HOCs exist as non-aqueous phase liquids (NAPLs) or are tightly adsorbed on the soil, which limits their distribution in the water phase and greatly hinders their effective treatment (Bueno-Montes et al., 2011; Liu et al., 2017a).

In the past few decades, surfactants have been widely used for the removal of HOCs from groundwater or soil (Huang et al., 2017; Zeng et al., 2018b). The micelles formed by surfactant are composed of an outer hydrophilic region and an inner hydrophobic core, which facilitates the partitioning of HOCs through the formation of surfactant/HOC aggregates (Trellu et al., 2016). These co-aggregates act as tiny HOCs reservoirs, which increase the apparent solubility of the HOCs and enhance the mass transfer of these contaminants in subsequent treatments, such as pump-and-treat (Higgins and Olson, 2009). This is the basis of surfactant-enhanced aquifer remediation (SEAR) technology, which is effective for the remediation of HOC-contaminated environments. However, surfactants have been reported to have harmful effects on human beings, to cause short- or long-term changes in the ecosystem (Lechuga et al., 2016), and to form difficult-to-separate emulsions (Malakootian et al., 2016) that may be bio-toxic to the environment (Long and Zhang, 2015). Therefore, the complete removal of the surfactant-HOC formations from the contaminated site after surfactant

Accepted MS

58 treatment is necessary. Although it has been reported that surfactant-solubilized HOCs
59 can be thoroughly removed by biological treatment (Zhu et al., 2010; Li et al., 2015),
60 sound data on bioremediation technology show that the effectiveness of microbes in the
61 degradation of contaminants depends on their microbiological activity and micro-
62 environment. Moreover, biological treatment often requires a long treatment period
63 (Kaczorek et al., 2013; Biswas et al., 2015).

64 An alternative technology which could be used to quickly and completely remove
65 surfactant-HOC formations from contaminated sites is advanced oxidation processes
66 (AOPs). AOPs are able to decompose nearly all types of organic pollutants into
67 harmless substances, and can be operated at or near ambient temperature and pressure
68 (Gong et al., 2009; Mantzavinos et al., 2017; Wang et al., 2019). Compared with
69 conventional chemical and biological processes, AOPs have the advantage of being
70 completely ‘‘environmentally-friendly’’, since they neither transfer contaminants
71 between phases (via process such as chemical precipitation or adsorption), nor produce
72 large amounts of hazardous sludge (Wang et al., 2018a; Wang et al., 2018b). AOPs
73 usually involve the in-situ generation of powerful oxidizing agents such as hydroxyl
74 radicals (•OH) (Cheng et al., 2018a; Zhou et al., 2018). In the past decades, the use of
75 AOPs for the pretreatment/treatment of surfactant-solubilized HOCs has been
76 suggested and investigated by many researchers. Huguenot et al. (2015) reported that
77 electro-Fenton treatment was successfully performed on the collected eluate of
78 petroleum-contaminated soil using Tween 80; the results demonstrated that the
79 mineralization ratio of the hydrocarbons was over 99.5% after 32 h. Long et al. (2013)
80 concluded that UV/$S_2O_8^{2-}$ oxidation was effective in the selective removal of toluene
81 (91%) and in the reuse of sodium dodecyl sulfate (SDS) from SDS soil flushing solution.

82 Fenton and Fenton-like processes each have their own unique advantages, which

Accepted MS

can include simple operation, high degradation efficiency and environmentally benign operation (Bendouz et al., 2017). During these processes, •OH can be continually produced via eq. (1) and (2) (Cheng et al., 2019):

$$Fe^{2+} + H_2O_2 \rightarrow Fe^{3+} + \bullet OH + OH^- \quad (1)$$

$$Fe^{3+} + H_2O_2 \rightarrow Fe^{2+} + HO_2\bullet + H^+ \quad (2)$$

Fenton oxidation has been used to treat a wide range of industrial wastewaters (Herney-Ramirez et al., 2010). However, the classical Fenton reaction has some disadvantages. For example, it is only efficient at low (~3) pH values (Zhou et al., 2014), and removal of the iron ions from the solution after the treatment process is difficult (Choi et al., 2014). To avoid these drawbacks, iron-containing solid heterogeneous Fenton-like catalysts have been developed (Tsai et al., 2011). Steel converter slag (SCS), a final waste material of the steel making process, has high potential as a heterogeneous catalyst in the Fenton-like process owing to its abundance of iron oxides; however, its use in this application is hindered by its high alkalinity (Cheng et al., 2016; Cheng et al., 2017). In this work, salicylic acid-methanol-acetone (SMA) solution was used to modify SCS, and the feasibility of using the SMA-modified SCS (SMA-SCS)/$H_2O_2$ Fenton-like system for the degradation of surfactant-solubilized HOCs was studied.

Rhamnolipid, one of the most important biosurfactants, is a promising alternative to synthetic chemical surfactants for SEAR due to its advantages, such as low toxicity and being environmentally friendly (Wu et al., 2015). More importantly, the solubilization capacity of rhamnolipid is superior to that of many synthetic surfactants (Ayed et al., 2015). This study focuses on the removal of rhamnolipid and rhamnolipid-solubilized hexadecane, a typical constituent of petroleum hydrocarbons, by the SCS-based heterogeneous Fenton-like system in aqueous solution. Alkanes make up 90% of petroleum hydrocarbons. *N*-hexadecane was selected as a model HOC because of its

Accepted MS

low solubility. According to our previous study, the measured solubility value of hexadecane in water is 0.00009 μM at 25 ℃. In the first step, the adsorption kinetics of rhamnolipids and hexadecane on SCS and SMA-SCS were studied. Subsequently, the effect of the rhamnolipid concentration on the degradation of hexadecane was evaluated. The changes in the hexadecane, rhamnolipid, and $H_2O_2$ concentrations, as well as in the pH value of the solution during the Fenton-like process, were also monitored. Finally, we performed continuous degradation experiments to verify the reusability of the SMA-SCS catalyst.

## 2. Materials and methods

### *2.1 Materials*

The SCS was kindly provided by Valin Iron and Steel Corp (VISTC), Xiangtan, China. The monorhamnolipid (rhamnolipid) biosurfactant (purity 99.9%) was purchased from Zijin Biological Technology Co. Ltd (Huzhou, China). The critical micelle concentration (CMC) of the rhamnolipid in mineral salt medium solution (MSM, composed of 0.5% $NH_4Cl$, 0.5% $Na_2HPO_4$, 0.25% $KH_2PO_4$, and 0.05% $MgSO_4 \cdot 7H_2O$; pH: ~6.0 (Liu et al., 2014)) was determined to be 83 μM (42 mg/L), based on the dependence of the MSM surface tension on the rhamnolipid concentration (Zhong et al., 2015a). Analytical grade hexadecane (purity ≥99%) was purchased from Sigma-Aldrich (St. Louis, MO., U.S.). Hydrogen peroxide ($H_2O_2$, 30% in water) was purchased from Sinopharm Chemical Reagent (Beijing, China). All other reagents were of chromatographic grade or analytical grade.

### *2.2 Preparation of rhamnolipid-solubilized n-hexadecane*

Two mL of *n*-hexadecane was pipetted into a 500-mL flask, and the flask was slowly rotated to ensure that the *n*-hexadecane was spread over the bottom of the flask. Then, 100 mL of MSM containing a predetermined concentration of rhamnolipid was

Accepted MS

added to the flask. This flask was cultivated in a reciprocal shaker at 30 ℃ and 100 rpm for 72 h, as our previous study showed that the solubilization equilibrium of *n*-hexadecane in rhamnolipid-MSM solution was obtained within 72 h (Zhong et al., 2014). The solution was then transferred into a separatory funnel and left to stand overnight. After phase separation had occurred, the aqueous phase was released from the bottom of the funnel at a steady and slow flow rate (about 1 drop/10 s) and collected. After repeating the above separation processes, the solution of *n*-hexadecane solubilized by rhamnolipid was obtained.

Three sets of MSM-based rhamnolipid-solubilized hexadecane solution were prepared. In (1), 50 mg/L of rhamnolipid was added to solubilize the hexadecane ($C_{50}$). In (2), the $C_{50}$ solution described in (1) was prepared, and then extra rhamnolipid was added to give a total rhamnolipid concentration of 200 mg/L. In (3), 200 mg/L of rhamnolipid was added to solubilizse the hexadecane ($C_{200}$).

*2.3 Preparation and characterization of the SMA-SCS catalyst*

The SMA solution was prepared by adding salicylic acid (50 g/L) to a 30:70 v/v methanol-acetone solution. The SCS powder was passed through a 0.15-mm mesh sieve washed using ultrapure water and then dried to a constant weight at 105 ℃ in an oven. Two g of dried SCS powder was added to 200 mL of SMA solution, and the flask was shaken on a shaking bed at 300 rpm and 25 ℃ for 4 h. The filtration residue was fully washed with ultrapure water and dried at 105 ℃ for 24 h after filtering the mixture using a 0.45 μm filter paper. The SMA solution modified-SCS (SMA-SCS) catalyst was obtained.

The Brunauer-Emmett-Teller (BET, TRI-STAR3020, USA) adsorption method was used to measure the specific surface area, pore volume, and pore size of the SCS and SMA-SCS. Surface properties were investigated using a scanning electron

Accepted MS

158 microscope (SEM) (Carl Zeiss, EVO-MA10, Germany) at a magnification factor of
159 1400. The components of SCS and SMA-SCS were analyzed using an Oxford energy
160 dispersive X-ray (EDX) detector. The crystal phases of SCS and SMA-SCS were
161 determined with a D/max-2500 X-ray diffractometer.

162 *2.4 Adsorption tests*

163 Adsorption experiments were carried out at a constant temperature (25 ℃) in 10-
164 mL plastic centrifuge tubes. Twenty mg of SCS or SMA-SCS and 1 mL of rhamnolipid-
165 solubilized hexadecane solution were added to each tube. These tubes were
166 immediately placed in a water bath shaker and shaken at 120 rpm. At predetermined
167 time intervals, several tubes were removed from the shaker and centrifuged at 1000 rpm
168 for 5 min. The hexadecane and rhamnolipid in the supernatant were extracted and
169 determined, respectively. The amount of adsorbate adsorbed on the catalyst ($Q_t$, mg/L)
170 was calculated using the following equation:

171 $$Q_t = (C_0 - C_t) \cdot V/m \quad (3)$$

172 Where $C_0$ is the initial concentration of the adsorbate (mg/L), $C_t$ is the measured
173 concentration of the adsorbate (mg/L), V is the volume of the reaction solution (L), and
174 m is the dry mass of the catalyst (g).

175 *2.5 Fenton-like process*

176 Ten-mL plastic centrifuge tubes were used as disposable reactors for the Fenton-
177 like reaction. Typically, 1 mL of rhamnolipid-solubilized hexadecane solution was
178 placed in the tube, and a certain amount (0.02 g) of SMA-SCS (or SCS) was added.
179 Then 0.03 mL of 30% $H_2O_2$ was added to the tube to start the degradation reaction. At
180 the beginning of the experiment, the tubes were immediately placed into a gyratory
181 shaker at 120 rpm and 25 ℃. At each predetermined time point, several tubes were
182 removed from the shaker, and 20 μL of ethanol was immediately added to quench the

Accepted MS

reaction in the tubes. The hexadecane, rhamnolipid, and $H_2O_2$ concentrations in the samples were analyzed. To acquire the hexadecane or rhamnolipid existing in the aqueous phase and on the solid surfaces, the extraction agents were added directly to the reaction tube. The pH value of the solution was also measured.

*2.6 Analytical methods*

The concentration of hexadecane was determined using gas chromatography (GC) (Liu et al., 2017a). In brief, 0.05 mL of 10% HCl solution, 2 mL of ethanol, and 1 mL of n-octane were added to the plastic centrifuge tube. After being vortexed for 5 min, the mixture was allowed to settle for 30 min. Then, a 2 mL sample of octane was collected from the upper phase and analyzed using an Agilent 6890N GC. The phenol-sulfuric acid method (Pinzon and Ju, 2009) was used to analyze the rhamnolipid concentration. First, the pH value of the sample was adjusted to 2.0 with 1 M HCl solution. Then, an equivalent of ethyl acetate was added to the plastic centrifuge tube and agitated for 5 min. After stratification, the organic phase was transferred to a new tube. This process was repeated three times, after which the acquired organic phase was dried at 60 ℃. Finally, the rhamnolipid solid was completely dissolved in 2 mL of 0.05 M $NaHCO_3$ solution, and then mixed sequentially with 1 mL of 5% phenol and 5 mL of concentrated sulfuric acid (98%). The concentration of rhamnolipid was determined using UV spectrophotometry (Shimadzu UV-2552) at 480 nm. $H_2O_2$ decomposition in the aqueous phase was measured using the $KMnO_4$-based titration method (Cheng et al., 2016). The pH value of the solution was determined using a Beckman 510 pH meter. All batch experiments were performed in triplicate. At each sampling point, three identical samples were withdrawn and results are presented as the mean ± standard deviation.

Accepted MS

## 3. Results and discussion

### *3.1 Characterization of SCS and SMA-SCS*

The SEM images (Fig. 1a and b) show that the untreated SCS particles have a relatively smooth, flat, and continuous surface. In comparison, SMA-SCS particles have more holes on the surface, which would increase their surface area and pore volume (Table S1), and thus enhance their catalytic activity in the Fenton-like reaction (Zheng et al., 2016). The results of the EDS-based surface elemental component analyses of the SCS and SMA-SCS are shown in Table S2 and Fig. S1. SMA treatment significantly changed the strength of the signals of the elements O, Ca, Fe, and Si via the selective removal of Ca and Si from the surface of SCS (Cheng et al., 2017). Therefore, after SMA modification, the percentage content of Fe in SCS showed an obvious increase, whereas the percentages of Ca and Si decreased.

Please insert Figure 1

The diffraction patterns of the SCS and SMA-SCS materials are shown in Fig. 1c. The compositional complexity of the SCS materials can be observed from their diffraction peaks ($2\theta$; 22.93 °-77.27 °). SMA modification significantly reduced the intensities of some peaks ($2\theta$; 29.41 ° and 60.80 °) assigned to tricalcium silicate (Camilleri et al., 2005) and several other peaks ($2\theta$; 32.08 °, 32.98 °and 47.52 °) assigned to dicalcium silicate (Liu et al., 2002). However, the intensities of the iron oxide peaks ($2\theta$; 33.70 °and 35.30 °) (Hu et al., 2010) were much higher than those of the SCS peaks in the SMA-SCS materials. The results verified that SMA modification did indeed selectively remove calcium silicate minerals from the SCS particles.

### *3.2 Adsorption kinetics*

The adsorption of organic pollutants onto the catalyst surface is important for the catalytic degradation reaction, since the heterogeneous Fenton-like degradation mainly

Accepted MS

232 occurs at the solid-liquid interface (Xie et al., 2014). An adsorption experiment was
233 performed to analyze the timescale of adsorption quantity of hexadecane and
234 rhamnolipid on the SCS and SMA-SCS particles, and the results are presented in Fig.
235 2a. Within the concentration range studied, the adsorption equilibrium of both
236 hexadecane and rhamnolipid on the two types of catalysts was nearly achieved within
237 30 min. The similar adsorption curves of hexadecane and rhamnolipid suggested that
238 they were adsorbed onto SCS and SMA-SCS in the form of a hexadecane/rhamnolipid
239 aggregate.

240 Please insert Figure 2

241 Pseudo-first-order and pseudo-second-order models (Cheng et al., 2018b) were
242 used to investigate the adsorption kinetics (Fig. 2b) and their respective equations are
243 as follows:

244 $$\log(Q_e - Q_t) = \log Q_e - k_f \cdot t/2.303 \quad (4)$$

245 $$t/Q_t = 1/k_s Q_e^2 + t/Q_e \quad (5)$$

246 Where $k_f$ and $k_s$ are the rate constants for the pseudo-first-order (1/h) and pseudo-
247 second-order (g/mg h) models, respectively. $Q_t$ and $Q_e$ are the adsorption quantities at
248 time t and at equilibrium (mg/g). The equations were fitted to the experimental data,
249 and the resulting parameters are summarized in Table 1. The correlation coefficients $R^2$
250 (for hexadecane, $R^2$ = 0.9954 and 0.9999; for rhamnolipid, $R^2$ = 0.9922 and 0.9999,
251 respectively) indicated that the pseudo-second order kinetic model showed better
252 agreement with the kinetic data, suggesting that chemisorption is the rate-limiting step

Accepted MS

253 during the process of hexadecane and rhamnolipid adsorption. For SMA-SCS, the
254 equilibrium adsorption capacities of hexadecane and rhamnolipid were 0.252 and 0.289
255 mg/g, respectively, which were significantly higher than those for SCS. The results
256 were consistent with the porous structure and higher specific surface area observed for
257 SMA-SCS.

258 Please insert Table 1

259 *3.3 Oxidative degradation of hexadecane solubilized by rhamnolipid*

260 The amount of soluble iron released and the surface area available for the catalytic
261 reaction both depend on the concentration of the catalyst in the heterogeneous Fenton-
262 like process (Arzate-Salgado et al., 2016; Liu et al., 2019). A wide range of SMA-SCS
263 amounts (from 0 to 20 g/L) were tested and the results are shown in Fig. 3. The
264 hexadecane removal ratio increased with increasing SMA-SCS concentration.

265 Please insert Figure 3

266 The hexadecane removal ratio is shown as a function of time in Fig. 4a. In both
267 the SMA-SCS and SCS systems, the rates of hexadecane degradation decreased with
268 time, and the reaction stopped after 18 h. This was likely due to the continuous
269 consumption of $H_2O_2$ during the reaction. For all three rhamnolipid-solubilized
270 hexadecane solutions, the hexadecane degradation rate and removal ratio achieved
271 using SMA-SCS as catalyst were higher than those of SCS. The results indicate that
272 SMA modification significantly enhanced the catalytic activity of SCS. This
273 enhancement probably occurred because SMA modification increased the specific
274 surface area as observed using BET analysis (Table S1), and provided more liquid–
275 solid interfacial sites for the oxidative dissociation (Pachamuthu et al., 2017).
276 Additionally, the removal of CaO from the surface of SCS by SMA treatment would

Accepted MS

277 expose more iron sites and enhance the iron content in the SCS.

278 Please insert Figure 4

279 Among the SMA-SCS-catalyzed solutions, a higher removal ratio of hexadecane
280 was observed in Solution (1), which contained hexadecane solubilized by 50 mg/L of
281 rhamnolipid, than in Solution (2), which contained the same concentration of
282 hexadecane but 200 mg/L of rhamnolipid. This result indicated that increasing the
283 rhamnolipid concentration inhibited the degradation of hexadecane. Based on classic
284 surfactant aggregation theories (Li and Chen, 2009; Liu et al., 2017b), when the
285 concentration is higher than CMC, surfactant monomers begin to aggregate and form
286 micelles consisting of a hydrophobic core and a hydrophilic shell. Furthermore, the
287 formation of hexadecane/rhamnolipid aggregates was detected via aggregate size
288 measurement using the dynamic light scattering (DLS) method, the results of which
289 demonstrated that the particle size stabilized when the rhamnolipid concentration was
290 increased above CMC (Zhong et al., 2015b). Therefore, it was speculated that high
291 concentrations of rhamnolipid may prevent hydroxyl radicals from coming into contact
292 with the solubilized hexadecane in the micellar cores. In addition, rhamnolipid
293 molecules may also compete with hexadecane for the oxidant, which would inhibit the
294 effective degradation of hexadecane. For example, the previous study suggested that
295 the competition of surfactants such as rhamnolipid can minimize the consumption of
296 •OH by the target compounds (Long and Zhang, 2015). This conclusion was in
297 agreement with that of Flotron et al. (2003), who found that the use of the surfactant
298 Brij-35 consumed some of the •OH during the Fenton reaction of three PAHs.
299 Additionally, in the Fenton-like reaction in Solution (3), which consisted of 200 mg/L
300 of rhamnolipid-solubilized hexadecane, the removal ratio of hexadecane was relatively
301 low in both the SCS and SMA-SCS systems, which suggests that a high concentration

Accepted MS

of hexadecane may have a negative effect on the degradation of the target pollutant.

*3.4 Response of rhamnolipid to oxidative degradation of hexadecane*

The degradation of rhamnolipid took place simultaneously with that of hexadecane in the SMA-SCS system (Fig. 4b). Interestingly, Mousset et al. (2014) studied the electro-Fenton (EF) degradation of soil-washing solutions heavily loaded with phenanthrene, and proposed •OH first degraded the surfactant micelles before degrading the phenanthrene molecules trapped in the micelle cores. In our experiment, however, the degradation of rhamnolipid was not preferential to that of hexadecane. This indicated that •OH might have higher oxidative activity towards the hexadecane enclosed in the rhamnolipid layer in the hexadecane/rhamnolipid aggregate in the SMA-SCS system. This was in agreement with the role of $SO_4^{\bullet-}$ in toluene removal observed by Long and Zhang (2015), who found that toluene in SDS/toluene flushing effluents could be selectively degraded by an electro/$Fe^{2+}$/persulfate process. Thus, it was hypothesised that •OH must first break the rhamnolipid layer, in order to access the solubilized hexadecane in the core area of the aggregates (Fig. 5). Further research is needed to clarify possible mechanisms. Overall, the results showed that the SMA-SCS/$H_2O_2$ method was efficient in the removal of solubilized hexadecane and a small amount of rhamnolipid. This phenomenon was in accord with the observation of Rosas et al. (2013), who employed Fenton oxidation to treat Tween 80-washed *p*-Cresol wastewater; their results demonstrated that Fenton oxidation selectively removed *p*-Cresol, and that the degradation of Tween 80 was lower than 10%.

Please insert Figure 5

*3.5 Variation of the pH and $H_2O_2$ concentration during Fenton-like process*

In the degradation experiment, the initial pH of the system was set as 6.0, because the pollutant solution always has a near-neutral pH value (Zhong et al., 2014). The

Accepted MS

change in the solution pH during the degradation process is shown in Fig. 6a. In a previous study, the pH value rapidly increased to pH 10 due to the dissolution of calcium minerals in SCS during the Fenton-like process, even when the initial pH value was adjusted to 3 (Cheng et al., 2016). However, only a slight increase in the pH was observed during the first 2 h in the experiment. The removal of CaO from the SCS via SMA modification and the buffering ability of the MSM solution may have been responsible for the relatively stable pH in the system. The stable pH could protect the Fenton-like reaction from the low oxidation potential of •OH, decomposition of $H_2O_2$, and deactivation of catalyst under alkaline conditions (Zhu et al., 2015), and thus may be beneficial for the effective degradation of hexadecane.

Please insert Figure 6

Fig. 6a shows that the pH value also increased slightly (from 6.0 to 6.7) with increasing reaction time in the three SMA-SCS systems. In contrast, in the traditional Fenton reaction, the pH of the wastewater decreases sharply because the Fenton reagents ($Fe^{2+}$ and $H_2O_2$) and most of the degradation products are intrinsically acidic (Sun et al., 2009). Additionally, heterogeneous Fenton-like processes have been reported to be inefficient at near-neutral pH conditions due to the existence of comparatively inactive iron oxo-hydroxides and the precipitation of iron ions as iron hydroxide (Malakootian et al., 2016; Zheng et al., 2016). However, the results in this experiment indicate that Fenton-like treatment can be performed at neutral pH with high degradation efficiency of the target pollutants when SMA-SCS is used as the catalyst.

The temporal changes in the $H_2O_2$ concentration during the Fenton-like process are presented in Fig. 6b. The concentration of $H_2O_2$, which was responsible for the degradation of hexadecane and rhamnolipid, decreased gradually for all three groups. After 16 h of treatment, the $H_2O_2$ was almost exhausted. The degradation rate of the

Accepted MS

compounds decreased with the consumption of $H_2O_2$.

*3.6 Environmental implications*

Fenton/Fenton-like processes are widely used for wastewater treatment. SCS, one of the main by-products of iron and steel industry, is more economical compared with the ferric salts used in the traditional Fenton reaction. Considering that most SCSs are used without taking full advantage of their properties at present, the use of SCS as a raw material to prepare catalysts for heterogeneous Fenton-like reactions may be an attractive option. SMA-SCS can catalyze the Fenton-like process at an almost-neutral pH. As shown in Fig. 6a, after the treatment, the pH value of decontaminated water demonstrated little change, which can avoid the environmental risks associated with acidic solutions. The versatility of this system is also enriched by the fact that the Fenton-like reaction preferentially degraded solubilized hexadecane over rhamnolipid, which allowed for potential rhamnolipid recovery. Additionally, there was no obvious loss (4.2%) in the catalytic activity of SMA-SCS after five successive degradation experiments, indicating its high recyclability (Fig. S2). The potential application of SCS in this field would offer a promising approach with environmental benefits.

**4. Conclusions**

An effective technology using SMA-modified SCS in a Fenton-like reaction for the treatment of rhamnolipid-solubilized hexadecane was investigated. Compared with those of SCS, the SMA-modified SCS material exhibited a higher surface area and more holes on its surface. The adsorption processes of both hexadecane and rhamnolipid fitted well to a pseudo-second-order-kinetic model. The removal efficiency of solubilized hexadecane in the SMA-SCS systems was significantly higher than that in SCS systems. About 81% and 36% of the hexadecane and rhamnolipid, respectively, were degraded during 24 h in the SMA-SCS system. It was hypothesized that the

Accepted MS

requirement for the •OH generated from SMA-SCS/$H_2O_2$ system to first break the rhamnolipid layer in order to access the solubilized hexadecane in core area of the aggregates was the reason for the co-degradation of rhamnolipid and hexadecane. SMA-SCS exhibited negligible deactivation (4.2%) over five reaction cycles. More importantly, the Fenton-like treatment using SMA-SCS as the catalyst can be performed at near-neutral pH with high hexadecane degradation efficiency. The results obtained in this study are of importance to the application of SMA-SCS as a catalyst in Fenton-like processes for the treatment of surfactant-solubilized HOCs.

**Acknowledgements**

This study was financially supported by the National Natural Science Foundation of China (51521006, 51378190, 51378192, 51670085), the Program for Changjiang Scholars and Innovative Research Team in University (IRT-13R17), China Postdoctoral Science Foundation Funded Project (2018M642977), Scientific Research Fund of Hunan Provincial Education Department (521293050).

**References**

Arzate-Salgado, S.-Y., Morales-Pérez, A.-A., Solís-López, M., Ramírez-Zamora, R.-M., 2016. Evaluation of metallurgical slag as a Fenton-type photocatalyst for the degradation of an emerging pollutant: Diclofenac. Catal. Today 266, 126-135.

Ayed, H.B., Jemil, N., Maalej, H., Bayoudh, A., Hmidet, N., Nasri, M., 2015. Enhancement of solubilization and biodegradation of diesel oil by biosurfactant from *Bacillus amyloliquefaciens* An6. Int. Biodeterior. Biodegrad. 99, 8-14.

Bendouz, M., Tran, L.H., Coudert, L., Mercier, G., Blais, J.-F., 2017. Degradation of polycyclic aromatic hydrocarbons in different synthetic solutions by Fenton's oxidation. Environ. Technol. 38, 116-127.

Biswas, B., Sarkar, B., Rusmin, R., Naidu, R., 2015. Bioremediation of PAHs and

Accepted MS

VOCs: Advances in clay mineral–microbial interaction. Environ. Int. 85, 168-181.

Bueno-Montes, M., Springael, D., Ortega-Calvo, J.-J., 2011. Effect of a nonionic surfactant on biodegradation of slowly desorbing PAHs in contaminated soils. Environ. Sci. Technol. 45, 3019-3026.

Camilleri, J., Montesin, F.E., Brady, K., Sweeney, R., Curtis, R.V., Ford, T.R.P., 2005. The constitution of mineral trioxide aggregate. Dent. Mater. 21, 297-303.

Cheng, M., Liu, Y., Huang, D., Lai, C., Zeng, G., Huang, J., Liu, Z., Zhang, C., Zhou, C., Qin, L., Xiong, W., Yi, H., Yang, Y., 2019. Prussian blue analogue derived magnetic Cu-Fe oxide as a recyclable photo-Fenton catalyst for the efficient removal of sulfamethazine at near neutral pH values. Chem. Eng. J. 362, 865-876.

Cheng, M., Zeng, G., Huang, D., Lai, C., Liu, Y., Xu, P., Zhang, C., Wan, J., Hu, L., Xiong, W., 2017. Salicylic acid–methanol modified steel converter slag as heterogeneous Fenton-like catalyst for enhanced degradation of alachlor. Chem. Eng. J. 327, 686-693.

Cheng, M., Zeng, G., Huang, D., Lai, C., Liu, Y., Zhang, C., Wan, J., Hu, L., Zhou, C., Xiong, W., 2018a. Efficient degradation of sulfamethazine in simulated and real wastewater at slightly basic pH values using Co-SAM-SCS /$H_2O_2$ Fenton-like system. Water Res. 138, 7-18.

Cheng, M., Zeng, G., Huang, D., Lai, C., Liu, Y., Zhang, C., Wang, R., Qin, L., Xue, W., Song, B., Ye, S., Yi, H., 2018b. High adsorption of methylene blue by salicylic acid–methanol modified steel converter slag and evaluation of its mechanism. J. Colloid Interface Sci. 515, 232-239.

Cheng, M., Zeng, G., Huang, D., Lai, C., Xu, P., Zhang, C., Liu, Y., Wan, J., Gong, X., Zhu, Y., 2016. Degradation of atrazine by a novel Fenton-like process and assessment the influence on the treated soil. J. Hazard. Mater. 312, 184-191.

Accepted MS

Choi, K., Bae, S., Lee, W., 2014. Degradation of pyrene in cetylpyridinium chloride-aided soil washing wastewater by pyrite Fenton reaction. Chem. Eng. J. 249, 34-41.

Cossaboon, J.M., Hoh, E., Chivers, S.J., Weller, D.W., Danil, K., Maruya, K.A., Dodder, N.G., 2019. Apex marine predators and ocean health: Proactive screening of halogenated organic contaminants reveals ecosystem indicator species. Chemosphere 221, 656-664.

Cui, X., Mayer, P., Gan, J., 2013. Methods to assess bioavailability of hydrophobic organic contaminants: Principles, operations, and limitations. Environ. Pollut. 172, 223-234.

Flotron, V., Delteil, C., Bermond, A., Camel, V., 2003. Remediation of matrices contaminated by polycyclic aromatic hydrocarbons: Use of Fenton's reagent. Polycyclic Aromat. Compd. 23, 353-376.

Gong, J.-L., Wang, B., Zeng, G.-M., Yang, C.-P., Niu, C.-G., Niu, Q.-Y., Zhou, W.-J., Liang, Y., 2009. Removal of cationic dyes from aqueous solution using magnetic multi-wall carbon nanotube nanocomposite as adsorbent. J. Hazard. Mater. 164, 1517-1522.

Herney-Ramirez, J., Vicente, M.A., Madeira, L.M., 2010. Heterogeneous photo-Fenton oxidation with pillared clay-based catalysts for wastewater treatment: A review. Appl. Catal., B 98, 10-26.

Higgins, M.R., Olson, T.M., 2009. Life-cycle case study comparison of permeable reactive barrier versus pump-and-treat remediation. Environ. Sci. Technol. 43, 9432-9438.

Hu, J., Shao, D., Chen, C., Sheng, G., Li, J., Wang, X., Nagatsu, M., 2010. Plasma-induced grafting of cyclodextrin onto multiwall carbon nanotube/iron oxides for

Accepted MS

adsorbent application. J. Phys. Chem. B 114, 6779.

Huang, K., Lu, G., Lian, W., Xu, Y., Wang, R., Tang, T., Tao, X., Yi, X., Dang, Z., Yin, H., 2017. Photodegradation of 4,4′-dibrominated diphenyl ether in Triton X-100 micellar solution. Chemosphere 180, 423-429.

Huguenot, D., Mousset, E., Van Hullebusch, E.D., Oturan, M.A., 2015. Combination of surfactant enhanced soil washing and electro-Fenton process for the treatment of soils contaminated by petroleum hydrocarbons. J. Environ. Manage. 153, 40-47.

Kaczorek, E., Sałek, K., Guzik, U., Dudzińska-Bajorek, B., Olszanowski, A., 2013. The impact of long-term contact of *Achromobacter sp.* 4(2010) with diesel oil – Changes in biodegradation, surface properties and hexadecane monooxygenase activity. Int. Biodeterior. Biodegrad. 78, 7-16.

Lechuga, M., Fernández-Serrano, M., Jurado, E., Núñez-Olea, J., Ríos, F., 2016. Acute toxicity of anionic and non-ionic surfactants to aquatic organisms. Ecotoxicol. Environ. Saf. 125, 1-8.

Li, F., Zhu, L., Wang, L., Zhan, Y., 2015. Gene expression of an *Arthrobacter* in surfactant-enhanced biodegradation of a hydrophobic organic compound. Environ. Sci. Technol. 49, 3698-3704.

Li, J.-L., Chen, B.-H., 2009. Surfactant-mediated biodegradation of polycyclic aromatic hydrocarbons. Materials 2, 76.

Lin, K., Liu, W., Gan, J., 2009. Oxidative removal of Bisphenol A by manganese dioxide: Efficacy, products, and pathways. Environ. Sci. Technol. 43, 3860-3864.

Liu, X., Tao, S., Ding, C., 2002. Bioactivity of plasma sprayed dicalcium silicate coatings. Biomaterials 23, 963-968.

Liu Y., Liu Z., Huang D., Cheng M., Zeng G., Lai C., Zhang C., Zhou C., Wang W.,

Accepted MS

Jiang D., Wang H., Shao B., 2019. Metal or metal-containing nanoparticle@MOF nanocomposites as a promising type of photocatalyst. Coord. Chem. Rev. 388, 63-78.

Liu, Y., Ma, X., Zeng, G., Zhong, H., Liu, Z., Jiang, Y., Yuan, X., He, X., Lai, M., He, Y., 2014. Role of low-concentration monorhamnolipid in cell surface hydrophobicity of *Pseudomonas aeruginosa*: Adsorption or lipopolysaccharide content variation. Appl. Microbiol. Biotechnol. 98, 10231-10241.

Liu, Y., Zeng, G., Zhong, H., Wang, Z., Liu, Z., Cheng, M., Liu, G., Yang, X., Liu, S., 2017a. Effect of rhamnolipid solubilization on hexadecane bioavailability: enhancement or reduction? J. Hazard. Mater. 322, 394-401.

Liu, Z., Yu, M., Zeng, G., Li, M., Zhang, J., Zhong, H., Liu, Y., Shao, B., Li, Z., Wang, Z., Liu, G., Yang, X., 2017b. Investigation on the reaction of phenolic pollutions to mono-rhamnolipid micelles using MEUF. Environ. Sci. Pollut. Res. 24, 1230-1240.

Long, A., Zhang, H., 2015. Selective oxidative degradation of toluene for the recovery of surfactant by an electro/$Fe^{2+}$/persulfate process. Environ. Sci. Pollut. Res. 22, 11606-11616.

Long, A., Zhang, H., Lei, Y., 2013. Surfactant flushing remediation of toluene contaminated soil: Optimization with response surface methodology and surfactant recovery by selective oxidation with sulfate radicals. Sep. Purif. Technol. 118, 612-619.

Malakootian, M., Jaafarzadeh, N., Dehdarirad, A., 2016. Efficiency investigation of photo-Fenton process in removal of sodium dodecyl sulphate from aqueous solutions. Desalin. Water Treat. 57, 24444-24449.

Mantzavinos, D., Poulios, I., Esplugas, S., An, T., Puma, G.L., Dionysiou, D.D., 2017.

Accepted MS

Emerging advanced oxidation processes for the elimination of micro-pollutants. Chem. Eng. J. 318, 1.

Mousset, E., Oturan, N., van Hullebusch, E.D., Guibaud, G., Esposito, G., Oturan, M.A., 2014. Influence of solubilizing agents (cyclodextrin or surfactant) on phenanthrene degradation by electro-Fenton process – Study of soil washing recycling possibilities and environmental impact. Water Res. 48, 306-316.

Pachamuthu, M.P., Karthikeyan, S., Maheswari, R., Lee, A.F., Ramanathan, A., 2017. Fenton-like degradation of Bisphenol A catalyzed by mesoporous Cu/TUD-1. Appl. Surf. Sci. 393, 67-73.

Pinzon, N.M., Ju, L.-K., 2009. Analysis of rhamnolipid biosurfactants by methylene blue complexation. Appl. Microbiol. Biotechnol. 82, 975-981.

Rosas, J., Vicente, F., Santos, A., Romero, A., 2013. Soil remediation using soil washing followed by Fenton oxidation. Chem. Eng. J. 220, 125-132.

Sun, J., Li, X., Feng, J., Tian, X., 2009. Oxone/$Co^{2+}$ oxidation as an advanced oxidation process: comparison with traditional Fenton oxidation for treatment of landfill leachate. Water Res. 43, 4363-4369.

Trellu, C., Mousset, E., Pechaud, Y., Huguenot, D., van Hullebusch, E.D., Esposito, G., Oturan, M.A., 2016. Removal of hydrophobic organic pollutants from soil washing/flushing solutions: A critical review. J. Hazard. Mater. 306, 149-174.

Tsai, T.T., Kao, C.M., Wang, J.Y., 2011. Remediation of TCE-contaminated groundwater using acid/BOF slag enhanced chemical oxidation. Chemosphere 83, 687-692.

Wang, H., Sun, Y., Wu, Y., Tu, W., Wu, S., Yuan, X., Zeng, G., Xu, Z.J., Li, S., Chew, J.W., 2019. Electrical promotion of spatially photoinduced charge separation via interfacial-built-in quasi-alloying effect in hierarchical $Zn_2In_2S_5/Ti_3C_2(O, OH)_x$

Accepted MS

527 hybrids toward efficient photocatalytic hydrogen evolution and environmental
528 remediation. Appl. Catal., B 245, 290-301.
529 Wang, H., Wu, Y., Feng, M., Tu, W., Xiao, T., Xiong, T., Ang, H., Yuan, X., Chew, J.W.,
530 2018a. Visible-light-driven removal of tetracycline antibiotics and reclamation of
531 hydrogen energy from natural water matrices and wastewater by polymeric carbon
532 nitride foam. Water Res. 144, 215-225.
533 Wang, H., Wu, Y., Xiao, T., Yuan, X., Zeng, G., Tu, W., Wu, S., Lee, H.Y., Tan, Y.Z.,
534 Chew, J.W., 2018b. Formation of quasi-core-shell $In_2S_3$/anatase $TiO_2$@metallic
535 $Ti_3C_2Tx$ hybrids with favorable charge transfer channels for excellent visible-
536 light-photocatalytic performance. Appl. Catal., B 235, 213-225.
537 Wu, W., Hu, Y., Guo, Q., Yan, J., Chen, Y., Cheng, J., 2017. Sorption/desorption
538 behavior of triclosan in sediment–water–rhamnolipid systems: Effects of pH, ionic
539 strength, and DOM. J. Hazard. Mater. 297, 59-65.
540 Wu, Y., Wang, Y., Huang, X., Simonnot, M.-O., Wu, W., Cai, X., Chen, S., Wang, S.,
541 Qiu, R., Zhang, W., 2018. Surfactant-facilitated dechlorination of 2,2′,5,5′-
542 tetrachlorinated biphenyl using zero-valent iron in soil/sediment solution:
543 Integrated effects of plausible factors. Chemosphere 212, 845-852.
544 Xie, Y., Yan, B., Xu, H., Chen, J., Liu, Q., Deng, Y., Zeng, H., 2014. Highly regenerable
545 mussel-inspired $Fe_3O_4$@ polydopamine-Ag core–shell microspheres as catalyst
546 and adsorbent for methylene blue removal. ACS Appl. Mat. Interfaces 6, 8845-
547 8852.
548 Zeng, Z., Liu, Y., Zhong, H., Xiao, R., Zeng, G., Liu, Z., Cheng, M., Lai, C., Zhang, C.,
549 Liu, G., Qin, L., 2018b. Mechanisms for rhamnolipids-mediated biodegradation
550 of hydrophobic organic compounds. Sci. Total Environ. 634, 1-11.
551 Zheng, J., Gao, Z., He, H., Yang, S., Sun, C., 2016. Efficient degradation of Acid

Accepted MS

552 Orange 7 in aqueous solution by iron ore tailing Fenton-like process. Chemosphere
553 150, 40-48.
554 Zhong, H., Jiang, Y., Zeng, G., Liu, Z., Liu, L., Liu, Y., Yang, X., Lai, M., He, Y., 2015a.
555 Effect of low-concentration rhamnolipid on adsorption of *Pseudomonas*
556 *aeruginosa* ATCC 9027 on hydrophilic and hydrophobic surfaces. J. Hazard.
557 Mater. 285, 383-388.
558 Zhong, H., Liu, Y., Liu, Z., Jiang, Y., Tan, F., Zeng, G., Yuan, X., Yan, M., Niu, Q.,
559 Liang, Y., 2014. Degradation of pseudo-solubilized and mass hexadecane by a
560 *Pseudomonas aeruginosa* with treatment of rhamnolipid biosurfactant. Int.
561 Biodeterior. Biodegrad. 94, 152-159.
562 Zhong, H., Yang, L., Zeng, G., Brusseau, M.L., Wang, Y., Li, Y., Liu, Z., Yuan, X., Tan,
563 F., 2015b. Aggregate-based sub-CMC solubilization of hexadecane by surfactants.
564 RSC Advances 5, 78142-78149.
565 Zhou, C., Lai, C., Huang, D., Zeng, G., Zhang, C., Cheng, M., Hu, L., Wan, J., Xiong,
566 W., Wen, M., Wen, X., Qin, L., 2018. Highly porous carbon nitride by
567 supramolecular preassembly of monomers for photocatalytic removal of
568 sulfamethazine under visible light driven. Appl. Catal., B 220, 202-210.
569 Zhou, L., Shao, Y., Liu, J., Ye, Z., Zhang, H., Ma, J., Jia, Y., Gao, W., Li, Y., 2014.
570 Preparation and characterization of magnetic porous carbon microspheres for
571 removal of methylene blue by a heterogeneous Fenton reaction. ACS Appl. Mat.
572 Interfaces 6, 7275-7285.
573 Zhu, L., Lu, L., Zhang, D., 2010. Mitigation and remediation technologies for organic
574 contaminated soils. Front. Environ. Sci. Eng. Chin. 4, 373-386.
575 Zhu, S.-N., Wang, C., Yip, A.C., Tsang, D.C., 2015. Highly effective degradation of
576 sodium dodecylbenzene sulphonate and synthetic greywater by Fenton-like

Accepted MS

577 reaction over zerovalent iron-based catalyst. Environ. Technol. 36, 1423-1432.

578

Accepted MS

**Figure captions:**

**Fig. 1** SEM images of the (a) SCS and (b) SMA-modified SCS, and (c) their XRD patterns.

**Fig. 2** Kinetics of the adsorption of hexadecane and rhamnolipid on the catalysts: (a) pseudo-first-order plots of adsorption, (b) pseudo-second-order plots of adsorption.

**Fig. 3** Effect of the amount of SMA-SCS used on the removal rate of the hexadecane solubilized by rhamnolipid during the heterogeneous Fenton-like treatment. Experimental conditions: $H_2O_2$ concentration = 3%; rhamnolipid concentration = 50 mg/L; temperature = 25 ℃; initial pH = 6.0.

**Fig. 4** Neutral pH condition studies of (a) solubilized hexadecane removal over the SCS and SMA-modified SCS and (b) rhamnolipid removal over the SMA-modified SCS catalyst. Experimental conditions: $H_2O_2$ concentration = 3%; catalyst loading = 20 g/L; temperature = 25 ℃; initial pH = 6.0.

**Fig. 5** Schematic of rhamnolipid-solubilized hexadecane oxidation in the SMA-SCS/$H_2O_2$ system.

**Fig. 6** Change in the (a) pH of the solution and (b) $H_2O_2$ concentration during the Fenton-like treatment catalyzed by SMA-SCS. Experimental conditions: $H_2O_2$ concentration = 3%; catalyst loading = 20 g/L; temperature = 25 ℃; initial pH = 6.0.

Accepted MS

598 **Table 1**

599 The calculated parameters of the pseudo-first and pseudo-second order kinetic models

| | | pseudo-first order | | | pseudo-second order | | |
|---|---|---|---|---|---|---|---|
| | | $Q_e$ (mg/g) | $k_f$ (1/h) | $R^2$ | $Q_e$(mg/g) | $k_s$(g/mg ħ) | $R^2$ |
| Hexadecane | SCS | 0.034 | 0.114 | 0.9143 | 0.038 | 2.02 | 0.9954 |
| | SMA-SCS | 0.227 | 0.119 | 0.9212 | 0.252 | 0.341 | 0.9999 |
| Rhamnolipid | SCS | 0.035 | 0.081 | 0.9224 | 0.040 | 1.58 | 0.9922 |
| | SMA-SCS | 0.258 | 0.082 | 0.9397 | 0.289 | 0.248 | 0.9999 |

600

601

Accepted MS

602 **Fig. 1**

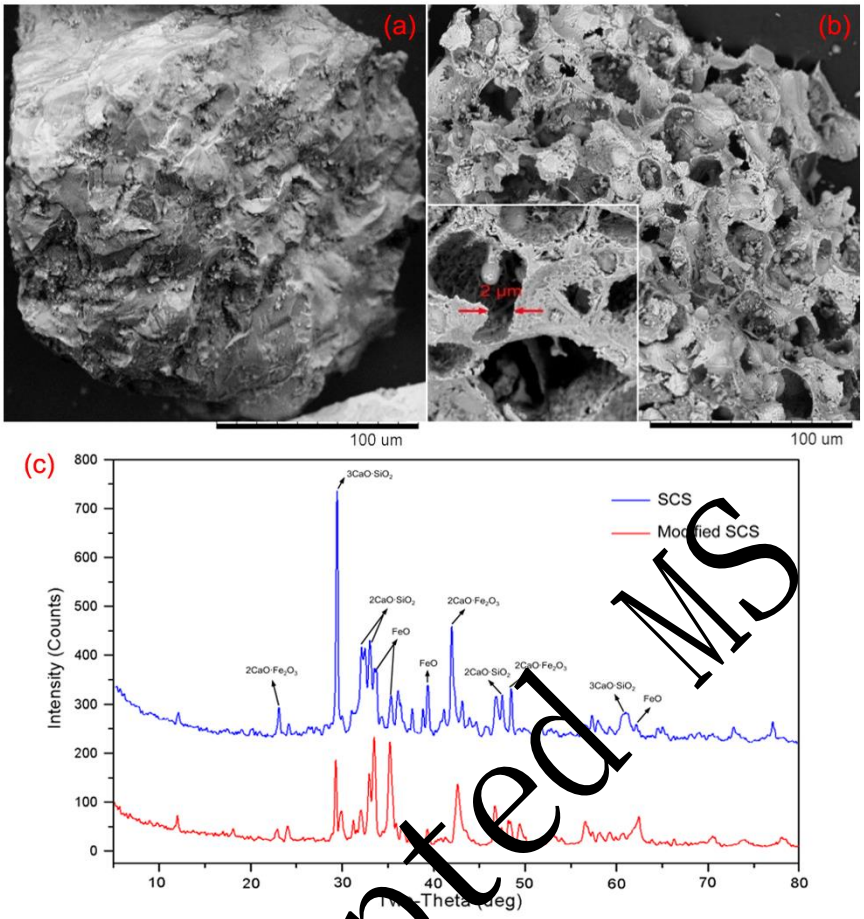


603

604

Accepted MS

605 **Fig. 2**

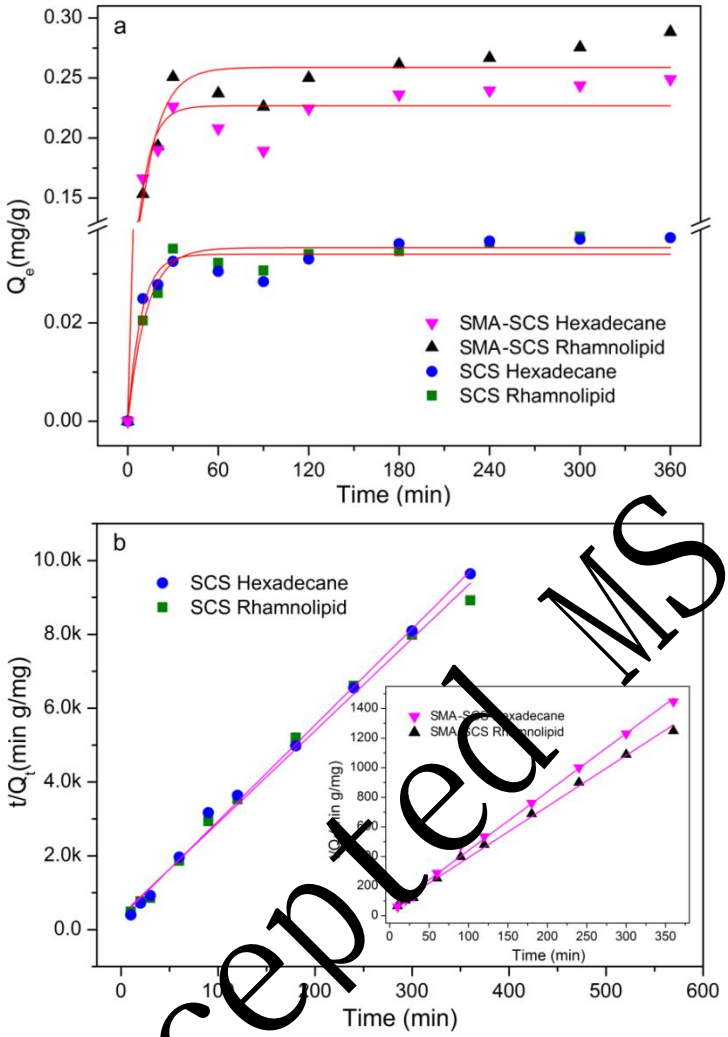


606

607

Accepted MS

608 **Fig. 3**

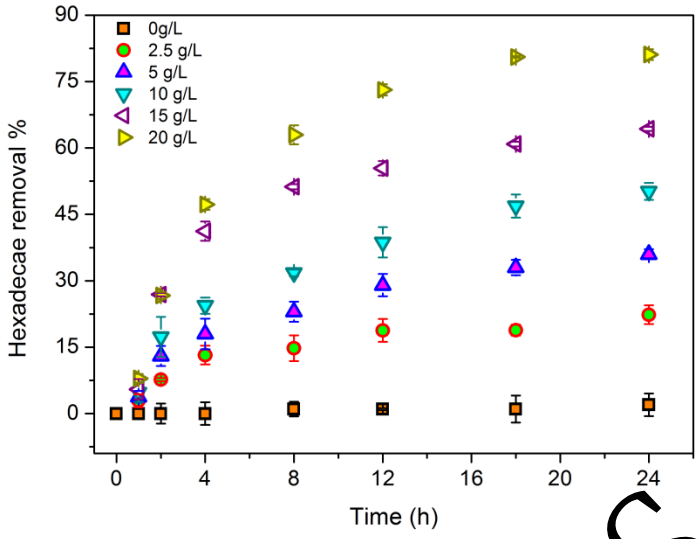


609

610

Accepted MS

611 **Fig. 4**

612 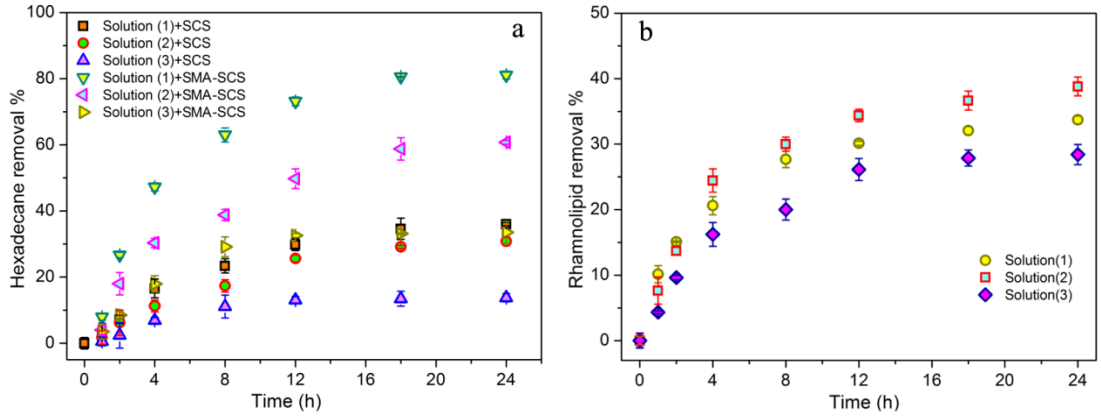


613

Accepted MS

614 **Fig. 5**

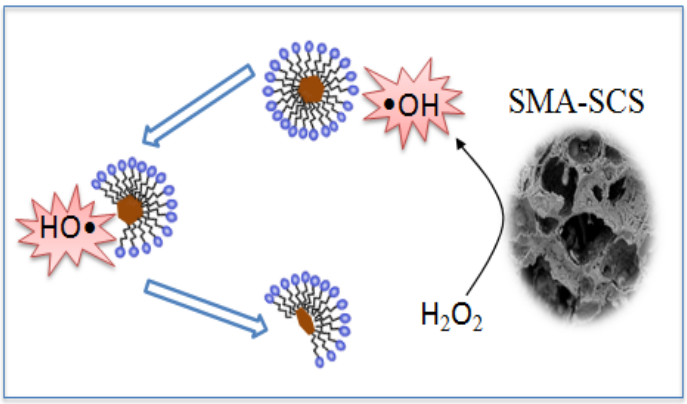


615

616

Accepted MS

617 **Fig. 6**

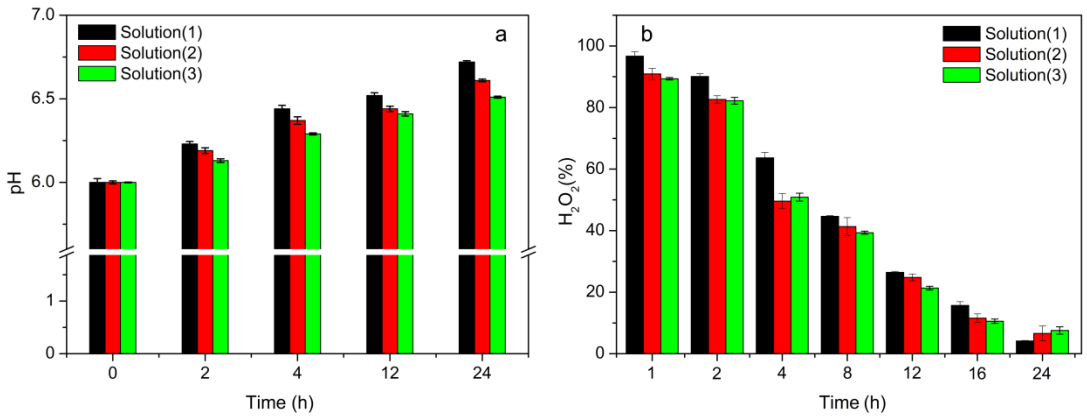


618

Accepted MS